Optimal Operation and Dispatch of Voltage Regulation Devices Considering High Penetrations of Distributed Photovoltaic Generation

Gyu-Jung Cho, Yun-Sik Oh, Min-Sung Kim, Ji-Soo Kim, Chul-Hwan Kim, Barry Mather, and Bri-Mathias Hodge

***Abstract*— Voltage regulation devices have been traditionally installed and utilized to support distribution voltages. Installations of distributed energy resources (DERs) in distribution systems are rapidly increasing, and many of these generation resources have variable and uncertain power output. These generators can significantly change the voltage profile for a feeder; therefore, in the distribution system planning stage of the optimal operation and dispatch of voltage regulation devices, possible high penetrations of DERs should be considered. In this paper, we model the IEEE 34-bus test feeder, including all essential equipment. An optimization method is adopted to determine the optimal siting and operation of the voltage regulation devices in the presence of distributed solar power generation. Finally, we verify the optimal configuration of the entire system through the optimization and simulation results.**

***Keywords*: IEEE 34-bus test feeder, distribution system planning, optimization, PV integration, step-voltage regulator**

I. Introduction

Voltage regulation devices such as capacitor banks or step voltage regulators (SVRs) have been installed and utilized for the improvement of the power factor or mitigation of voltage drops in current distribution system operational practice [1]–[2]. Recently, distributed energy resources (DERs) have begun to be extensively installed in the distribution system as auxiliary generation resources. The power output of renewable DERs is normally variable and uncertain because the characteristics of the input from the DERs are affected by the daily solar radiation or wind profile. If the distribution system operator plans to install new voltage regulation devices in the distribution system, it is clear that the output of the DERs will affect each device's location and operating schedule. Moreover, if the operator focuses on maximizing the DER capacity in the distribution system, the operation schedule or voltage device sizing and siting will be affected by the configuration of the DER installation and the resulting net load profile. Therefore, a study is needed on the optimal operation and dispatch of the voltage regulation devices that simultaneously considers the size of highly distributed DERs and the resulting net load profile.

Recently, several papers have addressed the optimization problem of the size and location of the capacitor banks [3]–[9] or the location and tap setting of the SVRs [10]–[13]. Many authors have focused on the performance of the optimization method. However, there have been very few optimization studies considering highly distributed DERs, the variable power output of the DERs, and the resulting operation of the voltage regulation devices simultaneously.

In this paper, we consider a monthly load profile from the summer of 2015 in Southern California. Open-source yearly solar radiation profiles from the National Renewable Energy Laboratory's National Solar Radiation Database (NSRDB) [14] are used to model the highly distributed photovoltaic (PV) generation. We utilize the IEEE 34-bus system as our target distribution system.

First, loads are allocated to the target distribution system based on a proportional representation from the original feeder load factors. 25 loads are individually placed on separate buses in the modified IEEE 34-bus test feeder, and each of the loads has a relevant profile according to certain criteria of the load capacity. The optimization variables—including the size and location of the PV, capacitor banks, and SVR settings—are assigned to the distribution system via the Open-Source Distribution System Simulator (OpenDSS) [15] using the COM interface. The optimization is performed by the Design Analysis Kit for Optimization and Terascale Applications (DAKOTA) [16]. The objective function values are calculated at every simulation iteration to evaluate the input parameters.

Finally, we utilize a quasi-static time-series (QSTS) simulation to consider the actual load and solar profiles to evaluate the monthly operation of the SVR, any voltage deviations, and the cumulative circuit power losses to calculate the constraints and economics of the system.

This work was partially funded by the U.S. Department of Energy under Contract No. DE_AC36-08-GO28308 with the National Renewable Energy Laboratory (NREL).

This work was supported by the National Research Foundation of Korea grant funded by the Korea government (No. 2015R1A2A1A10052459).

G. J. Cho, Y. S. Oh, M. S. Kim, J. S. Kim, and C. H. Kim are with the College of Information and Communication Engineering, Sungkyunkwan University, Suwon, 16419, Republic of Korea (e-mail: tom1220@skku.edu; fivebal2@skku.edu; michelle25@skku.edu; high7107@skku.edu; chkim@skku.edu).

B. Mather and B.-M. Hodge are with the Power System Design and Studies Group, NREL, Golden, CO 80401 USA (e-mail: Barry.Mather@nrel.gov; Bri.Mathias.Hodge@nrel.gov).

Paper submitted to the International Conference on Power Systems Transients (IPST2017) in Seoul, Republic of Korea, June 26–29, 2017

II. Target System and Equipment Topology

A. Quasi-Static Time-Series Simulation Based on the IEEE 34-Bus Test Feeder System

When a high penetration level of DERs is expected in a newly planned distribution system, power flow analysis of the target distribution system considering the cooperation among the voltage regulation devices, such as SVR and capacitor banks, is required to determine the optimal equipment dispatch as well as the operation schedule of the other devices. Because the QSTS simulation shows a series of simulation results of the static (snapshot) power flow results at each time step [17], it is well suited for these types of problems, and an appropriate time step that is able to accommodate the time interval for the operation of the power system equipment is needed.

In this paper, we use a modified IEEE 34-bus test feeder system and consider the actual load profile of a distribution feeder in Southern California. We use a monthly load profile from the summer of 2015 with solar radiation data added for distributed PV from the National Renewable Energy Laboratory's National Solar Radiation Database (NSRDB) [14].

B. Configuration of the Load and the PV Allocation

Fig. 1 shows the different types of the daily load profile and daily irradiance pattern from the NSRDB for an example day.

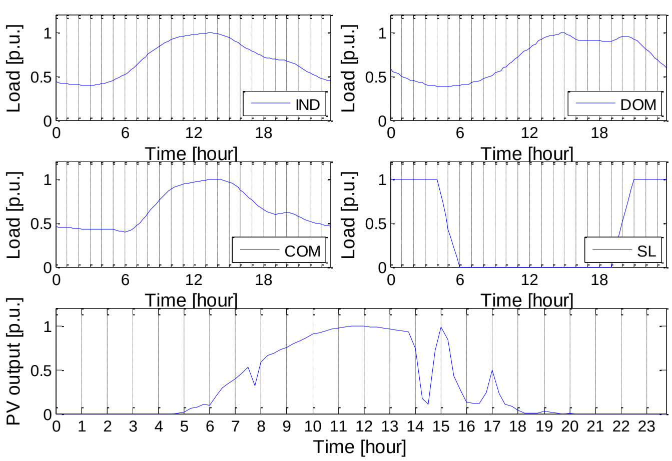

Fig. 1. Four types of load profiles and PV power output on June 30, 2015

We assume that each PV system is distributed with a rooftop configuration and that all of the PV systems are distributed throughout all of the load buses in the IEEE 34-bus test feeder system. A total of 25 buses among 56 buses (including the midpoint between each bus) of the target system are selected; the bus names, capacity of each load, and load types for each of the buses are shown in Table I. Four types of load profiles are adopted to consider the actual load pattern. The classified load types represent domestic single/multiple (DOM), small commercial (COM), industrial (IND), and street and area lightning (SL) load. The static load patterns of each load type can be obtained from [18]. Loads are dispatched in accordance with certain criteria of the load capacity [17]. The capacities of the PV systems are calculated according to the rating of the PV inverters. We assume that the PV inverters are rated at 120% of the maximum PV power output in peak radiation. The PV systems are assumed to be located at each of the 25 buses shown in Table I. The highlighted buses are locations where capacitor banks may be installed, as is introduced in the next section.

TABLE I
SIZES AND TYPES OF EACH LOAD

Bus Name	Load Size [kVA]	Load Type	Bus Name	Load Size [kVA]	Load Type
Mid806	84	DOM	Mid844	14	DOM
Mid810	24	DOM	844	720	IND
Mid824	7	SL	Mid846	68	DOM
Mid820	51	DOM	Mid848	34	DOM
Mid822	205	COM	848	108	IND
Mid826	60	DOM	Mid856	6	SL
Mid828	6	SL	Mid864	3	SL
Mid830	10	SL	Mid860	219	COM
830	65	DOM	860	108	IND
Mid858	22	DOM	Mid836	125	DOM
Mid834	49	DOM	Mid838	42	DOM
Mid840	60	DOM	890	675	IND
840	48	IND			

C. Configuration of the Voltage Regulation Devices

Fig. 2 shows a single-line configuration of the IEEE 34-bus test feeder system with the voltage regulation devices. There are two SVRs, and the operation of these devices will be defined by the setting of the target voltage of the SVRs and the band gap of the tap operation.

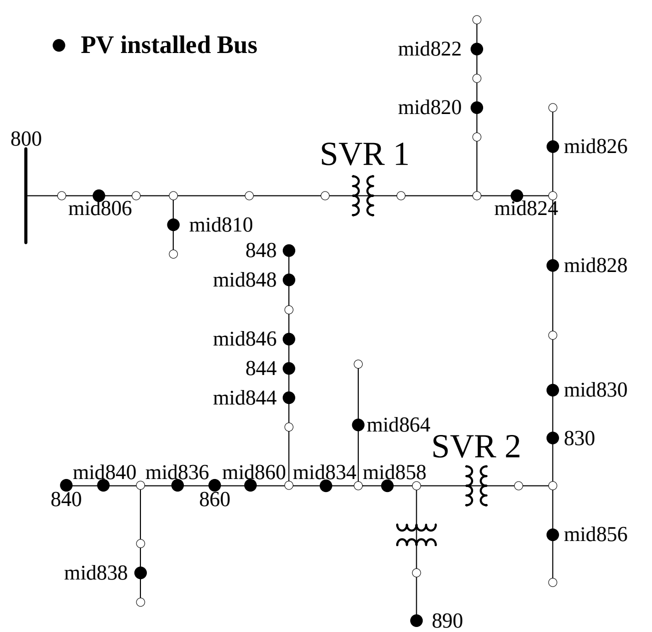

Fig. 2. Configuration of the IEEE 34-bus test feeder system

Seventeen buses of the IEEE 34-bus test feeder, where the capacitor banks can be installed, are chosen for the capacitor bank dispatching. There are three-phase loads on each bus, and these buses are highlighted in Table I. Two fixed-type capacitor banks are already installed in two of the buses of the original IEEE 34-bus test feeder system, 844 and 848; however, the size of these banks is quite large size compared to the size of the load at each bus, so a large amount of reverse reactive power flows in the lines adjacent to the two buses. To evaluate the test feeder, we eliminated the original two capacitor banks from the test feeder system. New capacitor banks, which have various sizes, will be dispatched to determine the optimal size and location of the capacitor banks according to the simulation conditions. Each capacitor bank is considered a fixed type because it has a relatively smaller size than the feeder transformer.

III. Optimal Operation and Dispatch of the Voltage Regulation Devices for Highly Distributed DERs

A. Problem Definition

A final purpose of the simulation is to determine the optimal capacity, siting of the capacitor banks, and the operational settings of the SVR. Table II shows the targets of the optimization to determine the optimal capacity and location of the newly installed capacitor banks considering highly distributed PV and the operation of the SVR.

TABLE II
TARGETS FOR THE OPTIMIZATION PROBLEM

Equipment	**PV**	**Allowable Range**
PV	Size	0–200 kVA
	Location	Every bus that has loads
Capacitor bank	Size	0–60 kvar
	Location	Every bus that has three-phase loads
SVR	Target voltage	120–128 V
	Tap band	1–6

The above parameters are used as inputs to the optimization problem. We change each parameter of the equipment as variables, and we evaluate each objective function at each simulation time step—i.e., every 15 minutes. Because the capacity of the PV and capacitor banks varies from 0 to 200 kVA or 60 kvar, we can effectively estimate the PV and capacitor bank installation. Through this, we can also evaluate the optimal location and the capacity of each piece of equipment to be located among the fixed target buses. In addition, we can estimate the SVR tap setting. Because various setting values are used for the simulation, the optimal set can be obtained from the simulation results.

Multiple objective functions are utilized because distribution planning, like most optimization problems, has many competing objectives. The three objective functions used in this work are defined in (1)–(3), where PV_i indicates the size of each PV; N is the total number of the installed PV systems; PF_{PV} is the average power factor of the whole PV during the simulation period; and C_{Cap}, C_{Loss}, and C_{SVR} calculate the maintenance cost due to the capacitor banks, circuit power loss, and SVR operation, respectively. Among these objective functions, F_1 and F_2 are to be maximized, whereas F_3 is to be minimized.

$$F_1 = \sum_{i=1}^{N} PV_i \tag{1}$$

$$F_2 = PF_{PV} \tag{2}$$

$$F_3 = C_{Cap} + C_{Loss} + C_{SVR} \tag{3}$$

Equation (1) represents the total size of the installed PV, and we aim to obtain the final PV hosting capacity (PVHC) of the system to the maximum extent possible. The purpose of this study is to determine the optimal operation of the voltage regulation devices in higher penetration levels of DER than general conditions; therefore, we maximize the PVHC as one of the objective functions, and we do not distinguish the penetration levels of the DER among each case. Equation (2) shows the average operating power factor of the whole system’s PV inverters. We adopt a simple power factor control algorithm to improve the power factor of the point of common coupling at the location of the PV installation. Equation (3) represents the total cost due to maintenance of each equipment and circuit power loss. It needs to be minimized to obtain a decreasing effect on the operating cost of the distribution system. We can calculate each term of (3) by following (4)–(6):

$$C_{Cap} = \sum_{i=1}^{M} \left(5.01 \times Q_i\right) \tag{4}$$

$$C_{Loss} = 0.075 \times P_{l,total} \tag{5}$$

$$C_{SVR} = \sum_{i=1}^{L} \left\{ Ca \times A^{-1}\left(i_a, T_e\right) + Cs \right\} \tag{6}$$

where M is the total number of the installed capacitor banks; Q_i is the size of each capacitor bank; $P_{l,total}$ is the total circuit power loss; Ca is the investment cost of the SVR; Cs is the maintenance cost of the SVR; and A^{-1} is a capital recovery factor, which is a function of annual interest rate and expected life of the SVR [11]–[12]. Each coefficient to calculate the cumulative cost of the capacitor banks and circuit power losses is considered [9].

Fig. 3 shows the flowchart of the optimization procedure. After the initialization, DAKOTA inputs an initial set of system parameters for the PVHC, capacitor banks, and SVR, as shown in Table II.

OpenDSS calculates the power flow during the simulation time step, which is 15 minutes in this study. Constraints for the voltage, conductor ampacity, and the reverse power flow are evaluated subsequently. Objective functions are calculated via the COM interface, and if there are any violations in the system, penalty values are added to the objective functions. Finally, DAKOTA resolves the optimization problem, which has multiple objective functions, by using a genetic algorithm. DAKOTA defines the best set of input variables—i.e., the size of the installed PV, capacity of each capacitor bank, and setting for each SVR in the system—according to the values of the three objective functions as measured by the OpenDSS QSTS simulations through an iterative process.

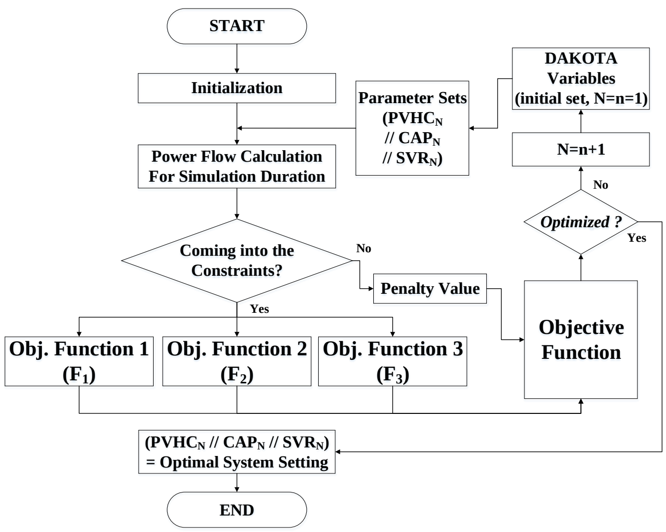

Fig. 3. Flowchart of the simulation procedure

B. Simulation Result: Overall

Fig. 4 shows the overall simulation results. The upper plot shows the relationship among the three objective functions; the lower plots verify the relationship between the PVHC and the other objective functions.

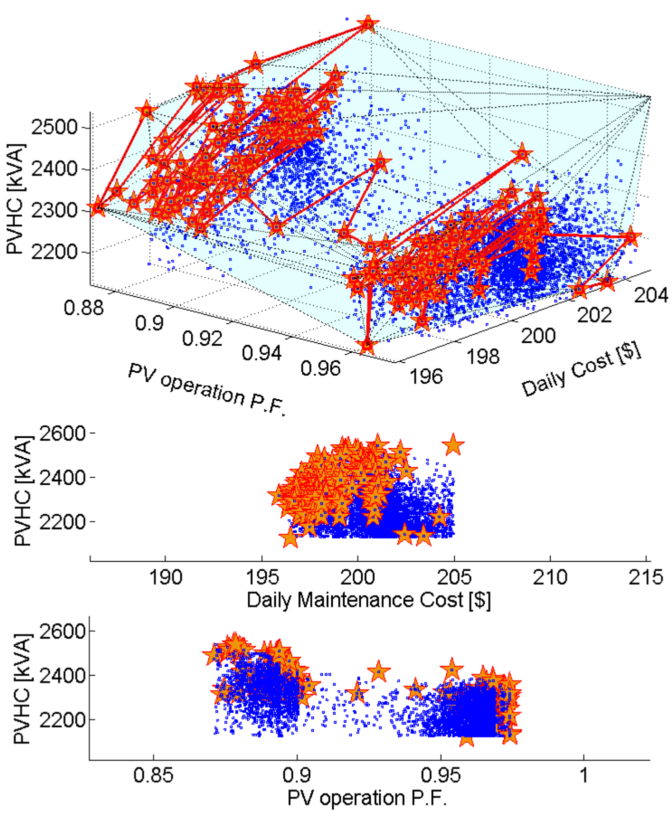

Fig. 4. Results of the overall simulation

Large stars in the figure denote feasible solutions on the Pareto optimal front, and the small dots represent other solutions tested during the optimization procedure. We obtained 158 Pareto optimal solutions from the simulation. We can draw the three-dimensional Pareto front approximately, which is highlighted by the bold line; and the Pareto surface, which is a three-dimensional convex hull shape.

Fig. 4 shows the tendency of each objective function. The results are divided into regions based on average operating power factor of the PV. If the distribution system has a purpose of dispatching a large amount PV, daily maintenance cost will be increased, and the PV operating power factor will be decreased. It seems that this trade-off means that the operation of the SVR is increased to maintain the overall voltage of the bus.

C. Simulation Result: Capacitor Banks

Fig. 5 shows the relationship between the total size of the installed capacitor banks and the daily maintenance cost; it is obtained from the parameter sets corresponding to feasible solutions on the Pareto surface. The filled triangles show results that are calculated in a condition such that the average PV operating power factor is less than 0.89. For the majority of the power factor values above 0.89, the total size of the capacitor banks should be increased to reduce the daily maintenance cost.

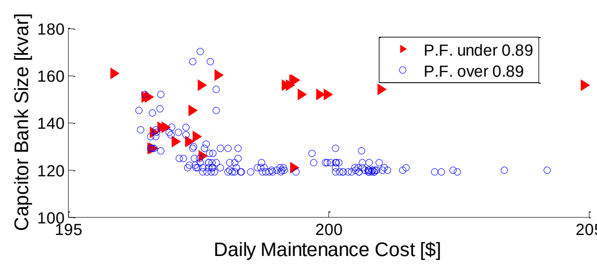

Fig. 5. Results of the capacitor bank size and daily cost

Fig. 6 shows the relationship between the PVHC and the total size of the capacitor banks. The straight line in the upper subplot represents a tendency of the PVHC according to the total size of the capacitor banks, which is shown in the lower subplot.

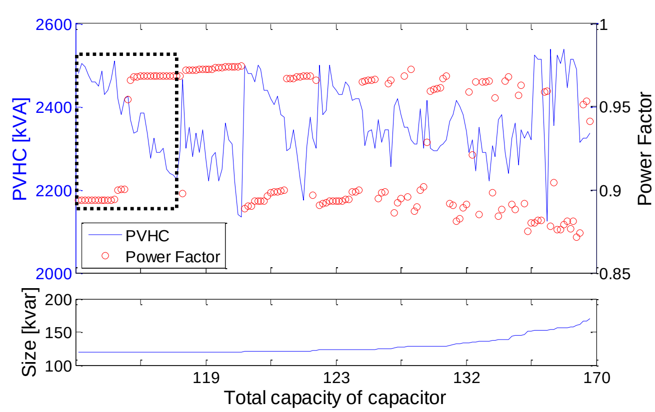

Fig. 6. Results of the capacitor bank size and other objective functions

The size of the installed capacitor banks does not seem to affect the PVHC of the distribution system; however, each capacitor bank has its own allowable PVHC, and it is affected by the PV operating power factor. For example, a dotted box in the upper subplot shows a result of the total of the 119-kvar capacitor banks. In this case, if the PV operating power factor maintains a high value, more than 0.95, the PVHC is decreased. As the PV operating power factor increases, this phenomenon becomes even worse. Therefore, if the objective is to operate PV in a high power factor, the trade-off relationship between PVHC and the PV operating power factor needs to be resolved to find the optimal values.

D. Simulation Result: SVR

Fig. 7 shows the relationship between the PVHC and the determined setting of each phase of the SVR. Three subplots in the first column represent the a, b, and c phase of SVR 1's optimized setting results, respectively; and the second column shows the same results for SVR 2.

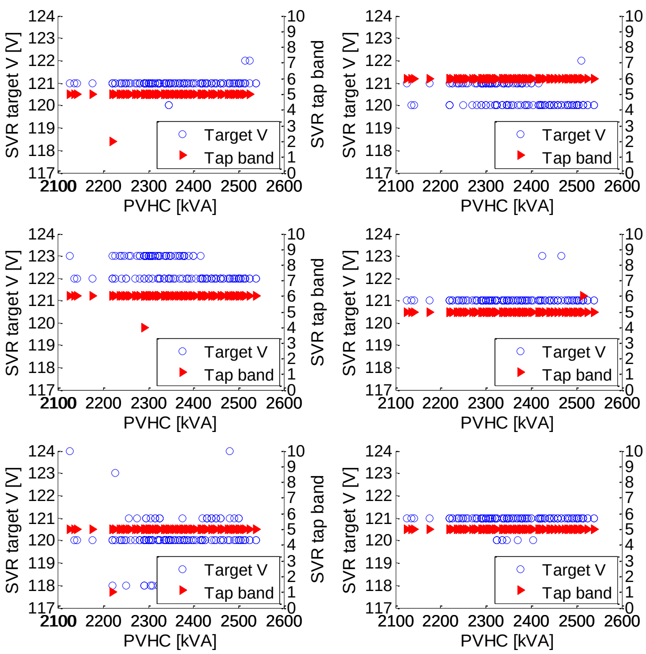

Fig. 7. Results of the SVR

Unlike the case of the capacitor bank, each setting value of the SVR is almost unchanged with the different amounts of PVHC, daily maintenance cost, and PV operating power factor. This means that the optimal setting values of each SVR can be fixed as a result.

E. Optimal Operation and Dispatch of the Voltage Regulation Devices

We can obtain possible optimal sets of the capacitor bank dispatch and the SVRs setting by considering the high penetration level of PV. We chose the two best cases based on the minimum daily maintenance cost. Fig. 8 shows the overall results of the installed PV and capacitor banks. According to the distance from the substation, the PV and capacitor banks show a similar tendency for each solution, respectively. In Bus 890, which experiences the most severe voltage drop, the PV and capacitor banks tend to be installed most frequently. In particular, the capacitor banks installed in each branch tend to be close to the substation, such as at buses 844 and mid840.

The optimal setting for each SVR is shown in Table III. Compared to the original setting value, the optimized tap band values tend to be widened, and the target voltages are slightly decreased. This result reflects the effect of cost due to the SVR operation, and it shows that the setting value of the SVR is optimized to reduce the number of tap-changing operations.

TABLE III
OPTIMIZED SETTING VALUES FOR EACH PHASE OF THE SVRS

	Original		**Best Solution**		**2nd Best Solution**	
	Target V [V]	**Tap Band**	**Target V [V]**	**Tap Band**	**Target V [V]**	**Tap Band**
SVR 1a	122	2	121	5	121	5
SVR 1b	122	2	123	6	123	6
SVR 1c	122	2	121	5	120	5
SVR 2a	124	2	121	6	121	6
SVR 2b	124	2	121	5	121	5
SVR 2c	124	2	121	5	121	5

The whole result shows a possible configuration of the voltage regulation devices with highly distributed PV in the IEEE 34-bus test feeder. Note that the result in this section focusses only on cost-effectiveness. In distribution system

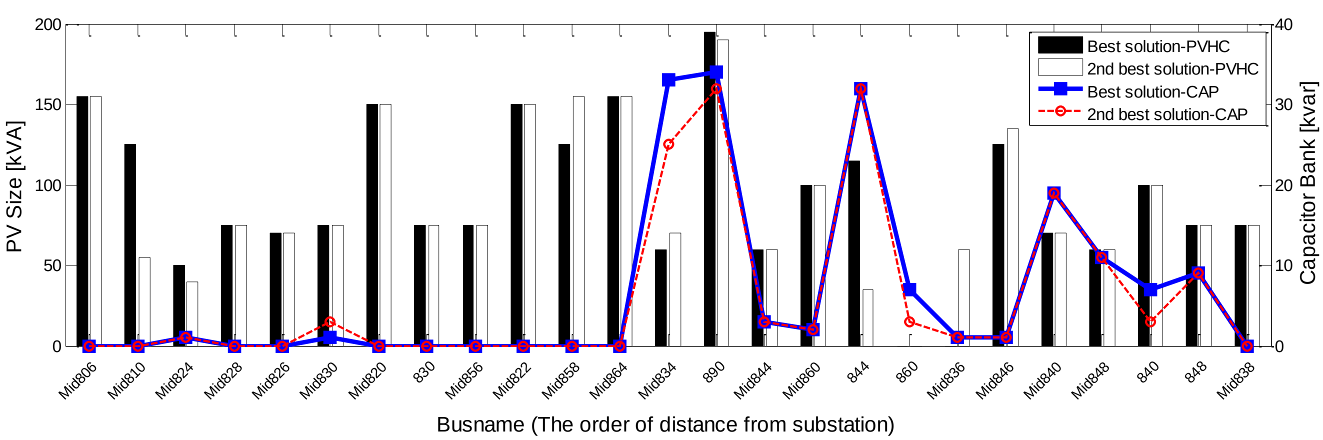

Fig. 8. Result plots of PVHC and capacitor banks size for the 2 best cases having cost-effectiveness

planning, the focus of the distribution system operator and the best solution sets will vary with the relevant aspects. Although we have been able to suggest a method to determine the optimal operation and dispatch of the voltage regulation devices through the optimization problem solving, an extended study is needed to reflect more realistic phenomena and the capacity of equipment.

IV. Conclusions

We have studied the optimal operation and dispatch of the voltage regulation devices using an optimization approach. The IEEE 34-bus test feeder was used as a test system, and modeling of the distribution system was performed by using OpenDSS with the COM interface. We used the DAKOTA program to resolve the optimization problem, and a genetic algorithm was used as the optimization method.

To drive the simulation model, we proposed an optimization problem with multiple objective functions, including PVHC, daily maintenance cost of the equipment, and the PV operating power factor. As a result of the simulation-optimization for the target distribution system, various Pareto sets were obtained. During the planning of a distribution system with a high penetration level of DERs, a simulation model such as that shown by the results of this paper can be used to understand the various trade-offs made in the design.

V. Acknowledgment

The U.S. Government retains and the publisher, by accepting the article for publication, acknowledges that the U.S. Government retains a nonexclusive, paid-up, irrevocable, worldwide license to publish or reproduce the published form of this work, or allow others to do so, for U.S. Government purposes.

VI. References

[1] T. Senjyu, Y. Miyazato, A. Yona, N. Urasaki, and T. Funabashi, "Optimal distribution voltage control and coordination with distributed generation," IEEE Trans. Power Del., vol. 23, no. 2, pp. 1,236–1,242, Apr. 2008.

[2] T. E. Grebe, "Application of distribution system capacitor banks and their impact on power quality," IEEE Trans. Ind. Appl., vol. 32, no. 3, pp. 714–719, Jun. 1996.

[3] R. A. Gallego, A. J. Monticelli, and R. Romero, "Optimal capacitor placement in radial distribution networks," IEEE Trans. Power Syst., vol. 16, no. 4, pp. 630–637, Nov. 2001.

[4] A. A. El-Fergany and A. Y. Abdelaziz, "Efficient heuristic-based approach for multi-objective capacitor allocation in radial distribution networks," IET Generation, Transmission & Distribution, vol. 8, no. 1, pp. 70–80, Jan. 2014.

[5] D. P. Montoya, J. M. Ramirez and J. R. Zuluaga, "Multi-objective optimization for reconfiguration and capacitor allocation in distribution systems," North American Power Symposium (NAPS), 2014, Pullman, WA, 2014, pp. 1-6.

[6] A. K. Fard and T. Niknam, "Optimal stochastic capacitor placement problem from the reliability and cost views using firefly algorithm," IET Science, Measurement & Technology, vol. 8, no. 5, pp. 260–269, Sept. 2014.

[7] M. B. Jannat and A. S. Savić, "Optimal capacitor placement in distribution networks regarding uncertainty in active power load and distributed generation units production," IET Generation, Transmission & Distribution, vol. 10, no. 12, pp. 3,060–3,067, Aug. 2016.

[8] Y. A. Baysal and I. H. Altas, "Cuckoo search algorithm for power loss minimization by optimal capacitor allocation in radial power systems," 2016 International Symposium on INnovations in Intelligent SysTems and Applications (INISTA), Sinaia, 2016, pp. 1–5.

[9] M. B. Jannat and A. S. Savić, "Optimal capacitor placement in distribution networks regarding uncertainty in active power load and distributed generation units production," IET Generation, Transmission & Distribution, vol. 10, no. 12, pp. 3,060–3,067, 2016.

[10] R. Shigenobu, A. Yona, T. Senjyu, and T. Funabashi, "Multi-objective optimization of SVR considering optimum placement and weather conditions in distribution systems," 2015 18th International Conference on Intelligent System Application to Power Systems (ISAP), Porto, 2015, pp. 1–6.

[11] A. S. Safigianni and G. J. Salis, "Optimum voltage regulator placement in a radial power distribution network," IEEE Trans. Power Syst., vol. 15, no. 2, pp. 879–886, May 2000.

[12] C. A. N. Pereira and C. A. Castro, "Optimal placement of voltage regulators in distribution systems," 2009 IEEE Bucharest PowerTech, Bucharest, 2009, pp. 1–5.

[13] B. A. Robbins, H. Zhu, and A. D. Domínguez-García, "Optimal tap setting of voltage regulation transformers in unbalanced distribution systems," IEEE Trans. Power Syst., vol. 31, no. 1, pp. 256–267, Jan. 2016.

[14] NREL Measurement and Data Center (MIDC) Solar Radiation Research Laboratory (SRRL) Baseline Measurement System (BMS), online resource: http://www.nrel.gov/midc/srrl_bms/, accessed Jan. 2017.

[15] OpenDSS electric power distribution system simulator, online resource: http://sourceforge.net/projects/electricdss/, accessed Oct. 2016.

[16] B. M. Adams, L. E. Bauman, W. J. Bohnhoff, K. R. Dalbey, M. S. Ebeida, J. P. Eddy, et al., "Dakota, a multilevel parallel object-oriented framework for design optimization, parameter estimation, uncertainty quantification, and sensitivity analysis: Version 6.4 user's manual," Sandia Technical Report SAND2014-4633, May 2016.

[17] B. A. Mather, "Quasi-static time-series test feeder for PV integration analysis on distribution systems," 2012 IEEE Power and Energy Society General Meeting, San Diego, CA, 2012.

[18] Southern California Edison, 2015 Static Load Profiles, online resource: https://www.sce.com/wps/portal/home/regulatory/load-profiles/, accessed Oct. 2016.